Vascular Engineering of Circulatory Assist Devices

13

Masahiro Nishida

Abstract

Heart failure is a condition in which the heart cannot pump sufficiently because its contractile force has deteriorated. Patients with heart failure can sometimes undergo heart transplantation, but in number these patients comprise less than 10 % of patients actually requiring heart transplantation. Thus, mechanical circulatory assistance plays an important role in substituting for heart transplantation wherein the pump function of the heart is assisted by an artificial blood pump called a ventricular assist device. On the other hand, cardiopulmonary bypass is a form of extracorporeal circulation that temporarily takes over the function of the heart and lungs to maintain the circulation of blood and the oxygen content of the body during surgery for heart failure and aneurysms of the thoracic aorta. This chapter describes the vascular engineering of circulatory assist devices. Particular emphasis is placed on recent progress in ventricular assist devices and cardiopulmonary bypass pumps. These important medical devices assist with human circulation at either the chronic or the acute phase. Because these devices are derived from an industrial pump, a great many studies have been conducted not only from the medical perspective but also from industrial and engineering perspectives. In this chapter, current ventricular assist devices and cardiopulmonary bypass pumps, their specifications, their classifications, and methods for their design and evaluating are presented, including flow analysis inside the pump to optimize the geometry.

Keywords

Ventricular assist device • Cardiopulmonary bypass pump • Pump design • Pump evaluation

M. Nishida (✉)
National Institute of Advanced Industrial Science and Technology, Tsukuba, Ibaraki, Japan
e-mail: masahiro.nishida@aist.go.jp

13.1 Introduction

This chapter describes the vascular engineering of circulatory assist devices. Particular emphasis is placed on recent progress in ventricular assist devices and cardiopulmonary bypass pumps. These important medical devices assist with human circulation at either the chronic or the acute phase. Because these devices are derived from an industrial pump, many studies have been conducted not only from the medical perspective but also from industrial and engineering perspectives. Some achievements have been commercialized; other designs are still being studied to confirm better compatibility or lifesaving capabilities for humans (Reul and Akdis 2000; Yamane 2002; Takatani et al. 2005; Joyce et al. 2012; Kyo 2014).

13.2 Ventricular Assist Device (VAD)

Heart failure, a condition in which the heart cannot pump sufficiently because of deterioration of its contractile force, is one of the most frequent causes of death in advanced countries. Patients with heart failure can sometimes undergo heart transplantation, but there are only about 4000 heart transplantations per year in Western countries, and only about 20 per year, including those as a passage, in Japan. Those numbers are less than 10 % of patients actually requiring heart transplantation. Thus, mechanical circulatory assistance plays an important role in substituting for heart transplantation in which the pump function of the heart is assisted by an artificial blood pump called a ventricular assist device (VAD). The main purpose of a VAD is as a bridge to heart transplantation. The waiting period for patients until heart transplantation is approximately 3 months, on average, in Western countries, and more than 1 year in Japan. At present, durability for longer than 5 years is required for all VADs. Further longer-term durability is desired for these devices, as the cases of destination therapy increase assuming long-term use of VADs for patients who cannot be adapted for heart transplantation. It is also necessary to enable long-term home medical care that is more adaptable to patients that are undergoing outpatient rehabilitation while maintaining the in-hospital function for patient management. Several things are essential for this purpose, such as an implantable pump, a portable driver, and a long-life battery.

13.2.1 Specifications of VADs

The flow rate of blood circulating in an adult at rest is 80 ml/min per 1 kg body weight, which means for a person weighing 60 kg, the blood flow rate is approximately 5 l/min and the pressure head of the heart is 100 mmHg. The target design parameters of a VAD, especially a left VAD, are usually defined as a flow rate of 5 l/min and a pressure head of 100 mmHg as average values. However, the natural pulsatile flow generated by a heart should be reflected in the pump flow because the VAD bypasses the left ventricle and aorta. Although the effect of the absence of
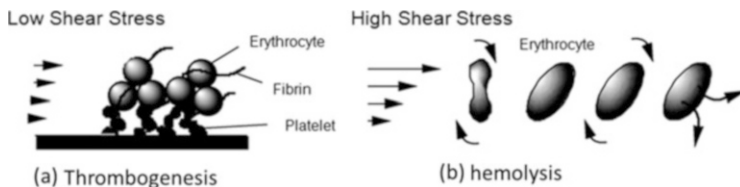
Fig. 13.1 Effect of flow on thrombogenesis and hemolysis

pulsatile flow on patients wearing continuous-flow VADs has been studied, long-term circulatory assistance was realized with continuous-flow VADs, and their effectiveness as well as that of wearing pulsatile-flow VADs, was verified by Golding et al. (1980).

The most important concern when designing VADs for long-term use is to prevent thrombus formation (blood coagulation). As thrombi usually form in areas where the shear rate is low (Fig. 13.1a), fluid dynamic design of the pump should prevent flow stagnation. More specifically, it is necessary to prevent areas of flow stagnation that cause thrombus formation, and the areas of flow stagnation should be washed out via shear stress on the surface of blood pumps. Another important aspect is prevention of hemolysis (erythrocyte fracture) caused by blood flowing through the pump. Under excessive shear stress, the erythrocyte membrane ruptures, and hemoglobin is released from the cells (Fig. 13.1b). Therefore, it is necessary to estimate the dynamic stimuli affecting erythrocytes and to design VADs that do not cause excessive shear stress.

13.2.2 Classification of VADs

13.2.2.1 Pulsatile-Flow VADs

Figure 13.2 shows various pulsatile-flow VADs. Two extracorporeal VADs [the Nipro VAD (Nipro, Japan (previously made by Toyobo, Japan)) and the Zeon VAD (Nippon Zeon and Aisin-seiki, Japan)] were covered under the health insurance system in Japan. These devices were pneumatic pulsatile-flow VADs, in which the blood is pumped via a diaphragm or sac motion caused by pneumatic pressure. At present, the Nipro VAD and the AB5000 (Abiomed, USA) are covered under the health insurance system as pulsatile-flow VADs in Japan. Pulsatile-flow VADs may be preferred from a physiological perspective, because they produce good clinical results, and the longest use has exceeded 3 years. However, these VADs require hospital management because they are extracorporeal VADs, which limits the activities of the patient, although the Movart NCVC (Senko Medical Instrument, Japan) is used with a portable compact driver that affords patients greater temporal mobility. Currently, pneumatic VADs are most often adapted as VADs for neonates and infants for reasons of their good hemocompatibility. Excor Pediatric (Berlin Heart, Germany) manufactures a number of different-sized pneumatic VADs.
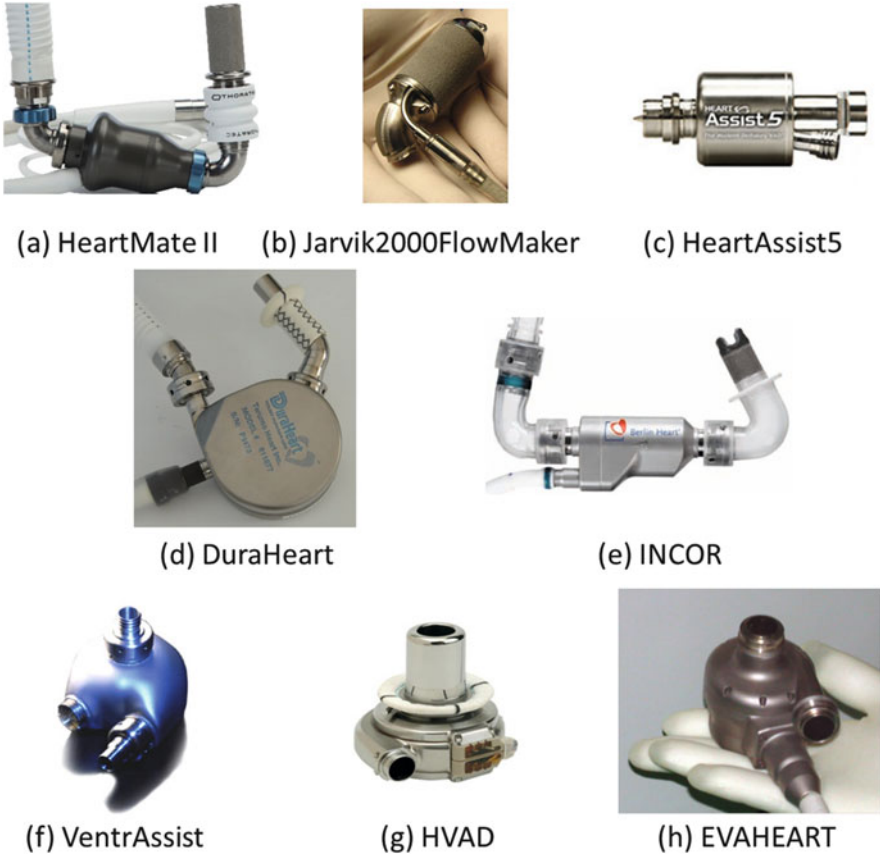
Fig. 13.2 Pulsatile-flow ventricular assist devices (VADs)

Two implantable VADs were used worldwide mainly in 1990s: the Novacor (World Heart, USA) and the HeartMate XVE (Thoratec, USA). Both are pulsatile-flow VADs that pump blood using a polyurethane blood sac moved by a magnetically driven pusher-plate and two artificial valves. These VADs have been used as the bridge to transplantation for more than 5000 patients worldwide because they dramatically improve the patients' quality of life. However, continuous-flow VADs, which are rotary pumps, have been developed because they are small, lightweight, and silent, and are expected to have longer-term durability. Pulsatile VADs are large and heavy (>1 kg), and the opening and closing of their valves is excessively noisy.

13.2.2.2 Continuous-Flow VADs

Figure 13.3 shows various continuous-flow VADs. These devices are presently the more widely implanted VADs because they have several advantages: a small size, no need for artificial valves, and increased reliability originating from their simple structure. The continuous-flow VADs originate from cardiopulmonary bypass (CPB) pumps used for heart operations. VADs are managed with the minimum use of anticoagulants because of the chronic use of the device, whereas CPB pumps are managed with the normal use of anticoagulants because these devices are used temporarily for a number of hours. Thus, anti-thrombogenicity is quite important for VADs. In light of this concern, development of continuous-flow VADs focuses on how the shaft and seal can be omitted or how the anti-thrombogenicity can be maintained around the bearing area at the center of rotation where the velocity is

(a) HeartMate II   (b) Jarvik2000FlowMaker   (c) HeartAssist5

(d) DuraHeart   (e) INCOR

(f) VentrAssist   (g) HVAD   (h) EVAHEART

Fig. 13.3 Continuous-flow VADs

very low. Determining how a large gap can be maintained between all material surfaces including the bearing gap in the pump is also important, not only because a large gap deceases hemolysis as a result of the decrease in high shear stress caused by a narrow gap, but also because it increases anti-thrombogenicity to secure the washout leakage flow around the center of rotation, which prevents the penetration of foreign substances from outside the pump.

Development of the HeartMate II (Thoratec) and the Jarvik2000FlowMaker (Jarvik Heart, USA) began at the end of the 1990s; these were the earliest among the various VADs available today. These early VADs were adapted for practical use and were heavily marketed as implantable VADs. Their axial-flow impellers are supported by two ball-cup bearings or pivot bearings. The advantage is the small size of the axial-flow pumps, which are $\phi 1.2$ in. $\times 2.8$ in. for the HeartAssist5 (MicroMed Cardiovascular, USA), $\phi 1$ in. $\times 2$ in. for the Jarvik2000FlowMaker, and $\phi 43$ mm $\times 81$ mm for the HeartMate II. The HeartAssist5 is used as a pediatric VAD. The disadvantage is that these axial-flow pumps have mechanical contacts, in

which the contact point in the blood-immersed structure should be washed out by the blood; this may decrease the hemocompatibility at that location.

To solve this problem, the magnetic levitation VAD and hydrodynamic levitation VAD were developed to achieve a non-contact impeller. Both types of VADs require the consideration of unbalanced forces and impeller weight for their design. VADs with magnetic bearings include the DuraHeart (Terumo, Japan), and the INCOR (Berlin Heart). In the DuraHeart, the centrifugal impeller is levitated using three-axis active controls, whereas in the INCOR the axial-flow impellers are levitated by active- and passive-axis controls. The advantage of the magnetic bearing is that it can have a large gap for hemocompatibility; however, it requires a sensor and control circuit for magnetic levitation.

VADs with a hydrodynamic bearing include the HVAD (HeartWare, USA) and the VentrAssist (Ventracor, Australia). Both these VADs adopt a tapered-land hydrodynamic bearing and centrifugal impeller. There is also a VAD with a hydrodynamic bearing that adopts the axial-flow impeller developed through collaboration with Mitsubishi Heavy Industries, the National Cerebral and Cardiovascular Center, and the National Institute of Advanced Industrial Science and Technology, Japan. The advantage of the hydrodynamic bearing is that it does not require a sensor or control circuit for levitation. On the other hand, the bearing is less hemocompatible because of its narrow bearing gap.

EVAHEART (Sun Medical Technology Research, Japan) adopts the mechanical journal bearing with the cool-seal system, which was originally developed to prevent thrombus formation via the circulation of pure water to wash the mechanical seal. The advantages of this VAD include no limit on the gap design and its small size, which result in good hemocompatibility, whereas the disadvantage is that it requires the maintenance-prone cool-seal system.

13.3   Cardiopulmonary Bypass (CPB) Pump

Cardiopulmonary bypass is a form of extracorporeal circulation that temporarily takes over the function of the heart and lungs to maintain the circulation of blood and the oxygen content of the body during surgery for heart failure and aneurysms of the thoracic aorta. Recently, the westernization of the everyday lifestyle in Japan has led to an increase in ischemic heart failure requiring coronary artery bypass surgery. Off-pump coronary artery bypass grafting tends to increase during coronary artery bypass surgery of the beating heart without extracorporeal circulation. Furthermore, there has been a recent focus on percutaneous surgery to expand the narrow segment of the coronary artery using a stent without opening the heart chamber. However, coronary artery bypass surgery with extracorporeal circulation and valvular disease of the heart require opening the chambers of the heart, and this necessitates extracorporeal circulation via cardiopulmonary bypass.

Extracorporeal circulation and blood oxygenation have been experimentally investigated since the nineteenth century. Gibbon was the first to successfully utilize cardiopulmonary bypass for an animal during general perfusion in 1937

(Gibbon 1937), and also the first to successfully utilize cardiopulmonary bypass for direct visual repair of an arterial septal defect in 1953 (Gibbon et al. 1953). The latter half of the twentieth century saw remarkable developments in cardiopulmonary bypass support for heart surgery. The types of adaptable patients expanded from only infants and adults to neonates and elderly people, and the target diseases changed from simple to complicated and severe. The survival rate for patients undergoing cardiopulmonary bypass is increasing dramatically.

The main setup for cardiopulmonary bypass consists of an oxygenator, a heat exchanger, a cooling water supply system, pump, circuit, reservoir, and an artery filter. Here, focus is placed on the pump.
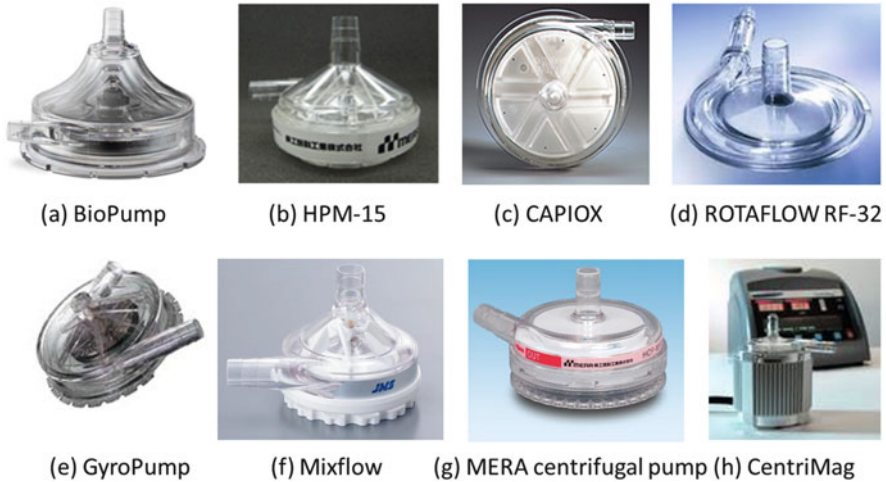
13.3.1 Specifications of CPB Pump

There are roller pumps and centrifugal pumps for the CPB pump. The roller pump is commonly used, and the centrifugal pump is used when the flow rate is higher than 2 l/min because it is difficult to control a flow rate lower than 0.5 l/min with these pumps.

13.3.1.1 Roller Pump

A roller pump was developed for transfusion by DeBakey in 1934 (DeBakey 1934). In principle, the roller rotates to massage tubing peristaltically and gently propels the blood through the tubing. This pump is commonly used for cardiopulmonary bypass because of its simple structure, robustness, simple operation, and reliability. Current pumps use two rollers, and the tubing is made of soft polyvinyl chloride resin. Initially, there was concern regarding peripheral circulatory failure as tissue perfusion is performed by nonphysiological blood flow. Later, however, 4–5 h of tissue perfusion by extracorporeal circulation with a roller pump was found to be without problems. The pump is now used safely for open-heart surgery.

13.3.1.2 Centrifugal Pump

A centrifugal blood pump was developed by Rafferty in 1968 (Rafferty et al. 1968). This pump ultimately became a commercialized pump named the "BioPump" in 1976. The impeller rotates at a rotational speed of several thousand revolutions per minute. Negative pressure is generated at the pump inlet (impeller rotational center), and positive pressure is generated at the pump outlet (impeller circumference) according to the spiral principle. Although a roller pump has been mainly used for open-heart surgery, the use of a centrifugal pump is gaining impetus. One of the reasons is because centrifugal pumps idle even if there is no blood in the pump, thus eliminating the possibility of air bubbles.

(a) BioPump   (b) HPM-15   (c) CAPIOX   (d) ROTAFLOW RF-32

(e) GyroPump   (f) Mixflow   (g) MERA centrifugal pump (h) CentriMag

Fig. 13.4 Cardiopulmonary bypass (CPB) pumps

13.3.2 Classification of CPB Pumps

The CPB pumps usually use magnetic coupling by which the rotating force of the motor is transferred to the impeller in the pump head; this facilitates easy pump head change without any direct connection.

Figure 13.4 shows various CPB pumps. A journal bearing with a seal and a pivot bearing are usually used for CPB pumps. The BioPump (Medtronic) uses a journal bearing with a seal and pumps blood by rotation of a cone-shaped impeller. The HPM-15 (Senko Medical Instrument Manufacturing, Japan), and the CAPIOX (Terumo) use a ball bearing with a seal and pump blood by rotation of an impeller with blades. The RotaFlow RF-32 (Maquet, Germany), the MERA centrifugal pump (Senko Medical Instrument Manufacturing), the GyroPump (Medtronic), and the Mixflow (JMS, Japan) use pivot bearings. The RotaFlow RF-32 and the MERA centrifugal pump use a single pivot bearing and a centrifugal impeller, whereas the GyroPump and the Mixflow use double pivot bearings. The GyroPump uses a centrifugal impeller and the Mixflow uses a mixed-flow impeller. Currently, the magnetic bearing is used in the CentriMag (Thoratec) as a CPB pump.

13.4 Design of Continuous-Flow Pump

The pump performance required for a continuous blood pump is classified into several types by the purpose. The main uses are generally for the VAD, the CPB pump, the extracorporeal membrane oxygenation (ECMO) pump, and the percutaneous cardiopulmonary support (PCPS) pump. The VAD is an implantable or extracorporeal independent pump, whereas the CPB, ECMO, and PCPS pumps

Table 13.1 Typical clinical driving conditions of blood pumps for an adult

Condition	VAD	CPB	ECMO	PCPS
Pressure (mmHg)	100	350	325	500
Flow rate (l/min)	5	5	0.5	3

are extracorporeal multipurpose pumps. The essential driving condition of blood pumps is achieved by satisfying the pump performance, as shown in Table 13.1 (Kawahito and Nosé 1997).

13.4.1 Impeller

Centrifugal and axial-flow impellers are used in rotary blood pumps to increase the pressure by rotation. For an impeller with diameter D, a rotational speed n, and an impeller tip speed u, the flow rate Q is

$$Q \sim D^2 u \sim nD^3, \tag{13.1}$$

and the head H is

$$H \sim u^2 \sim n^2 D^2. \tag{13.2}$$

When the left side is a constant multiple of the right side in both equations, both velocity and pressure distributions are similar. Omitting D from these equations,

$$\frac{n\sqrt{Q}}{H^{3/4}} \equiv n_S \tag{13.3}$$

becomes constant. Here, n_s is the specific speed, and is a parameter used to determine impeller types that exhibit similarities in their pumping even if the pump sizes are different. In this article, the dimensioned specific speed based on the units of "rpm, m³/min, m" is used, although the dimensionless specific speed $(= n\sqrt{Q}/(gH)^{3/4})$ is used worldwide, where g is the gravitational force. Figure 13.5 shows the relationship between the impeller geometry and the specific speed. The practical range of the centrifugal impeller is $80 < n_s < 1400$, which shows good efficiency in the low flow rate region. On the other hand, the practical range of the axial-flow impeller is $n_s > 600$, which shows good efficiency in the high flow rate region (Stepanoff 1957).

To set a pressure of 100 mmHg and a flow rate of 5 l/min for a VAD, the practical impeller rotational range of the centrifugal impeller is $1,400 < n < 25,000$ rpm, and that of the axial-flow impeller is more than 10,000 rpm in terms of efficiency. Here, the leakage flow should be secured to achieve adequate shear stress in the blood pump, which is sometimes realized by an adequate leakage flow with a large gap to wash out around the rotational center
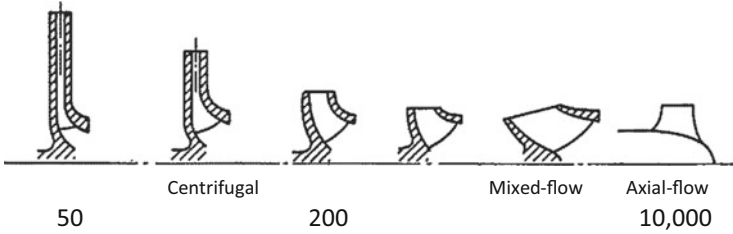
Fig. 13.5 Impeller geometry and specific speed
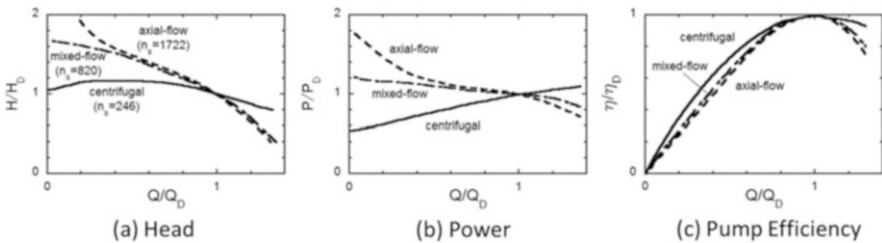
**Fig. 13.6** Typical pump performance classified by impeller geometry

including bearings where stagnation tends to occur. The leakage flow is large, and usually becomes more than 1 l/min when the pump flow rate is 5 l/min.

The pump performance is closely related to the impeller geometry, which is characterized by the specific speed. Figure 13.6 shows typical pump performance classified by impeller geometry. The pressure head and power dramatically increase around the no-discharge input where the flow rate is 0 for the axial-flow impeller whose specific speed is large, because backward flow is generated when the flow rate decreases. Conversion of the mechanism to that of the centrifugal impeller increases the pressure head, and work against the backward flow increases the power. On the other hand, the head and power smoothly vary for the centrifugal impeller with a low specific speed, because the small backward flow only increases to a large backward flow when the flow rate decreases without any mechanism change.

Another important aspect about impeller geometry is that it governs the anatomical fit of the blood pump, especially for implantable VADs. The inflow is in the direction of the rotational axis, and the outflow is in the direction vertical to the rotational axis and is apart for the impeller radius from the rotational axis. On the other hand, both the inflow and the outflow are in the direction of the rotational axis in the axial-flow impeller.

13.4.2 Bearing

The bearing supports the rotating axis of the impeller. The various kinds of bearings for rotary blood pumps include journal bearings, pivot bearings, hydrodynamic bearings, and magnetic bearings (Fig. 13.7). Although a ball bearing is popular for industrial use, it is not used for a rotary blood pump because it has a short life at a high rotational speed. Tables 13.2 and 13.3 show mechanical elements of CPB pumps and VADs, respectively, which include not only the bearing but also the relationship of rotor and impeller, and the coupling.
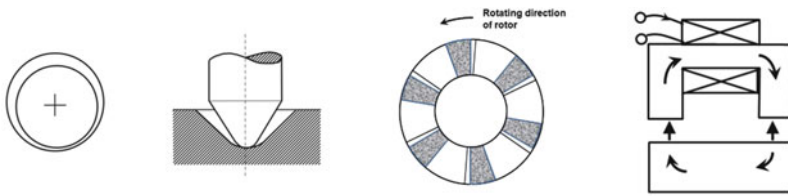
(a) Journal bearing (b) Pivot bearing (c) Hydrodynamic bearing (d) Magnetic bearing

Fig. 13.7   Bearings

Table 13.2   Mechanical elements of cardiopulmonary bypass (CPB) pumps

Product	Rotor and impeller	Coupling	Bearing
BioPump	Separated	Magnetic coupling	Journal bearing and seal
HPM-15, CAPIOX	Separated	Magnetic coupling	Ball bearing and seal
RotaFlow, MERA centrifugal pump	Separated	Magnetic coupling	Pivot bearing (single)
GyroPump, Mixflow	Separated	Magnetic coupling	Pivot bearing (double)
CentriMag	Unified	No coupling	Magnetic bearing

Table 13.3   Mechanical elements of VADs

Product	Rotor and impeller	Coupling	Bearing
HeartMate II, Jarvik2000FlowMaker	Unified	No coupling	Pivot bearing (double)
HVAD, VentrAssist	Unified	No coupling	Hydrodynamic bearing
DuraHeart	Separated	Magnetic coupling	Magnetic bearing
EVAHEART	Separated	Connected by shaft	Hydrodynamic journal bearing (with cool-seal system)

13.4.2.1 Journal Bearing

A journal bearing has a simple structure, a shaft inserted into a hole. It achieves stable rotation with the support of a heavy weight. It also allows for a considerably free design of the impeller, as other bearings must have a narrow gap between an impeller and a casing. However, a seal is required to prevent blood leakage. Thus, considering hemocompatibility, a journal bearing is usually used for short-term use blood pumps, such as a CPB pump, because thrombus formation might occur around the gap if blood penetrates the gap between the shaft and the seal. For long-term use, a special anti-thrombogenicity design is required for the seal around the bearing. The BioPump, the HPM-15, and the CAPIOX use this bearing for CPB pumps, and the EVAHEART uses this bearing for a VAD. For long-term use, the EVAHEART uses a hydrodynamic journal bearing with the cool-seal system. In the cool-seal system, pure water continuously washes the mechanical seal to prevent blood from penetrating into the seal gap, which could lead to thrombus formation.

13.4.2.2 Pivot Bearing

A pivot bearing consists of a pivot shaft and an end stone that only make contact at a single point. The possibility of thrombus formation is considerably low, as the contact area in the bearing is minimized. However, the wash around a pivot bearing is important to increase its hemocompatibility, as it is not a non-contact bearing. Various improvements are made to the wash around the pivot bearing, and the wear of the bearing is also investigated. There is a single pivot type that supports only behind the impeller and a double pivot type that supports both in front of and behind the impeller. The RotaFlow and the MERA centrifugal pump are single pivot-type bearings for CPB pumps. The single pivot type is driven under the condition that the positive thrust force is loaded on the end stone. Thus, the force is adjusted with the magnetic attraction force of the magnetic coupling. Here, the fluid force should be considered, which is usually a negative thrust force, because the pressure is high in the outlet and low in the inlet. As for pumps that use double pivot-type bearings, there are the GyroPump and the Mixflow as CPB pumps and the HeartMate II and the Jarvik2000FlowMaker as VADs. The double pivot-type stably rotates with high bearing stiffness, but it has two bearings, which might increase the possibility of thrombus formation.

13.4.2.3 Hydrodynamic Bearing

A hydrodynamic bearing considerably increases hydrodynamic force by special grooves in the blood pump, although, overall, it is the same classification as that of a sliding bearing including a journal bearing, etc. The HVAD uses this bearing. The mechanism of the hydrodynamic bearing involves generating pressure by thrusting the fluid into the gap by viscous force when two planes move, and the geometry gradually narrows in the moving direction.

13.4.2.4 Magnetic Bearing

A magnetic bearing uses a feedback control system where coiled magnetic iron cores face the center rotor, and the rotor is supported by the magnetic attractive

force. There is no wear on the bearing, as it achieves non-contact support that ensures high hemocompatibility. The CentriMag uses this bearing for a CPB pump and a short-term VAD, and the DuraHeart uses this bearing for a VAD.

13.5   Evaluations of Continuous-Flow Pump

The evaluations of VAD are overall established by the International Organization for Standardization (ISO) Standard for circulatory support devices. The ISO 14708-5 specifies the requirements for safety and performance of active implantable circulatory support devices. To satisfy the ISO 14708-5, the Japanese R&D guidance for VAD and total artificial heart were published by the Ministry of Economy, Trade and Industry, that describes the pump performance test including fluid dynamics analysis of blood pump, the hemolysis test, the animal test, the durability test, and many other tests of developing VADs (ISO 14708–5 2010; Imachi and Mussivand 2010; Yamane et al. 2010).

13.5.1 Pump Performance Measurement

The pump performance measurement of rotary pumps follows ISO 5198, "Centrifugal, mixed flow and axial flow pumps — Code for hydraulic performance tests — Precision grade" (ISO 5198 1987).

13.5.2 Hemolysis Test

The hemolysis evaluation follows ASTM F1841-97, "Standard practice for assessment of hemolysis in continuous flow blood pumps" (ASTM F1841-97 1997).

13.5.3 Animal Test (Anti-thrombogenesis Test)

The protocol with adequate consideration for the purpose of system use and patient safety, raw data, the observed record, and explanation and consideration of the results should be described. There must not be severe thromboembolism that is considered to have originated in the apparatus. Here, "severe" is defined as events that threaten animal life or cause conditions to deteriorate. The suspected cases of severe thromboembolism should be monitored by medical practitioners for deterioration in conditions such as the clinically unacceptable dysfunction of the kidneys or liver, as is previously defined, uncontrolled pain with any analgesic administration or analgesia treatment, and paralysis requiring assistance resulting from condition deterioration. Regular observations should be based on medical practice and diagnosis. There is currently no consensus on the appropriate number and period of animal experiments. However, it is preferable that sufficient evidence is provided

that enables progression to a clinical study, with the results from animal experiments that are conducted with six animals for more than 60 days, or eight animals for more than 90 days, corresponding to the purpose of use.

13.5.4 Durability Test

The purpose of the durability test is to prove that there is no problem in the system, including reliability in daily use based on risk analysis, etc. The target patients depend on the condition that an applicant describes as the purpose of use. The fundamental goal is to record and report all events. Whether the test is stopped or continued when events occur needs to be determined. The system reliability is expressed by the number of tests and the number of failures to validate the function as intended within the specifications (period and environment) that an applicant determined. Namely, the number of test apparatuses that are necessary to attain the reliability and the confidence level is set. At least 6 months of testing are required with 80 % reliability and a 60 % confidence level for the experimental condition and the period of the durability test. Table 13.4 shows the number of tests with 80 % reliability and an 80 % confidence level, and Table 13.5 shows the number of tests with different confidence levels. A 6-month test is recommended with 80 % reliability and an 80 % confidence level when considering international harmonization. It is preferable to continue the test for more than 2 years. Test conditions are set by considering the instrument properties. It is recommended that the environment of the durability test be determined by considering physiological condition and life pattern such as pressure, flow rate, pulsatility, pH, temperature, and electrolytes.

Table 13.4 Number of tests with 80 % reliability and 80 % confidence level

Assumed number of failures	Reliability and confidence level	Number of tests
No failure allowed	80 %, 80 %	8
One failure allowed	80 %, 80 %	14
Two failures allowed	80 %, 80 %	21

Table 13.5 Number of tests with different confidence levels (Pantalos et al. 1998, Yamane et al. 2010)

Recommender	Reliability and confidence level	Number of tests (1 failure allowed)
ASAIO-STS	80 %, 60 %	9
Japanese R&D Guidance	80 %, 70 %	11
	80 %, 80 %	14
	80 %, 90 %	18

13.6 Fluid Dynamics Analysis of Blood Pump

Pump performance and hemocompatibility are important design indices in the development of blood pumps. Therefore, blood pumps were conventionally designed based on basic pump design theory, and focus was placed on avoiding flow stagnation to prevent thrombus formation and excessive high shear to prevent hemolysis. The performance was evaluated through repeated performance tests, hemolysis tests, and anti-thrombogenesis tests with animals to confirm design validation. However, in addition to the conventional methods, the inner flow state is grasped in more recent methods for developing blood pumps, even if only roughly, and is used for fluid dynamic design of the inner geometry of blood pumps because the pump performance and hemocompatibility are strongly related to the flow. The pump design is required to achieve an inner flow that avoids both excessive high shear regions and stagnation regions because hemolysis occurs in excessive high shear regions and thrombogenesis occurs in regions of stagnant flow in the blood pump. Therefore, the load of various tests related to fluid dynamics has been lightened by fluid dynamics analysis. The analyses described concern pump performance, hemolysis, anti-thrombogenesis and impeller levitation, which are considered important aspects in developing blood pumps. Discussions of various results from tests that have been conducted blindly, especially the discussions about blood test results, are supported by engineering, and the speed at which blood pumps are developed has consequently increased. Table 13.6 shows various flow analyses and their properties of methods, which can be used as follows.

(a) Computational fluid dynamics analysis

Computational fluid dynamics (CFD) analyses are used to analyze flow in blood pumps. There are now many CFD studies because of the recent development and popularity of commercial software, which makes the analysis easy for researchers who do not specialize in this type of analysis. The advantage of CFD analysis is to

Table 13.6 Properties of flow analysis methods

	Advantage	Disadvantage
Computational fluid dynamics	Easy output of various physical property (e.g., path line), simultaneous pressure analysis	Validation requirement of accuracy, difficulty for too complicated flow (e.g., flow in pulsatile-flow pump)
Qualitative flow visualization	Easy, low cost	No quantification
LDV measurement, hot-wire velocimetry	Precise, good traceability on flow	One-point measurement, error near the surface wall, high cost
PIV measurement	Multipoint measurement, high space resolution	High cost

be able to grasp easily the overall flow. However, the accuracy of CFD analysis should be validated by experimental fluid dynamics analysis, as it is not guaranteed, because geometric approximation is necessary when generating meshes, and because the most appropriate analysis method (solution method, turbulent model, etc.) is not determined at present.

(b) Qualitative flow visualization

Qualitative flow investigations that have been conducted on the inner flow of blood pumps and that are not accompanied with velocity quantification are called flow visualization (Affeld et al. 1976). Typical methods are the tracer injection method and the surface trace method. The streak line method (Schima et al. 1992) and the suspension method (Araki et al. 1993) are examples of the tracer injection method, and the oil dot method (Burgreen et al. 2001) and the oil film method (Tsukiya et al. 2002) are examples of the surface trace method. Qualitative flow visualization is sometimes conducted on the inner flow because overall goodness can be judged for the geometry design of blood pumps. For example, one can judge whether there is vortex or separation in the flow between blades of an impeller or in the flow between the impeller and the outlet by the suspension method. Moreover, one can judge whether there is stagnation in the flow in the pump by the oil dot and oil film methods. Thus, qualitative flow visualization is a meaningful experimental analysis. It has a reliability that the CFD analysis cannot achieve, and it not only reduces the work required for quantification and error estimation, but also reduces the cost for the experimental apparatus.

(c) Laser Doppler velocimetry and hot-wire velocimetry measurements

Laser Doppler velocimetry (Pinotti and Paone 1996) and hot-wire velocimetry (Chua et al. 2002) are methods for measuring the inner flow of the blood pump. These methods are well known to be highly precise in spite of the disadvantage of being labor intensive from the one-point measurements, because the tracer invasiveness is small and time resolution is high. Therefore, these methods are used for measurements that require high precision.

(d) Particle image velocimetry measurement

Particle image velocimetry (PIV) quantifies particle images obtained by the suspension method because qualitative methods cannot calculate quantitative values such as velocity, shear rate, shear stress, etc. In the 1990s, flow was analyzed in axial-flow blood pumps to improve the pump performance, which depends on the blade geometry (Kerrigan et al. 1996). However, the PIV measurement method was not adapted to analyze the flow in the axial-flow blood pump because it was difficult to assess three-dimensional flow by measuring the particle motion on a laser-light sheet. On the other hand, there are many adaptations of PIV measurement to analyze flow in the centrifugal blood pump (Ikeda et al. 1996; Nishida et al.

1999) because the main flow and secondary flow, which is a sub-flow perpendicular to the main flow, are usually two-dimensional flows.

13.6.1 CFD Analysis

In this section, current CFD analyses are described, which are established as an important development tool to optimize the geometry of blood pumps.

13.6.1.1 Methodology of CFD

The equations governing flow are the conservation equations of mass, moment, and energy that correspond to the continuity equation, the momentum equation, and the energy equation, respectively. The CFD analysis calculates the flow field by which these equations are discretized and algebraically solved (Japan Society of Mechanical Engineers 1988). A flow field and translated fluid dynamic values from the flow field in the blood pump, which are required for development of the blood pump, are calculated through the same process as CFD analysis of the flow in a general pump. Figure 13.8 shows the typical process of blood pump development using CFD
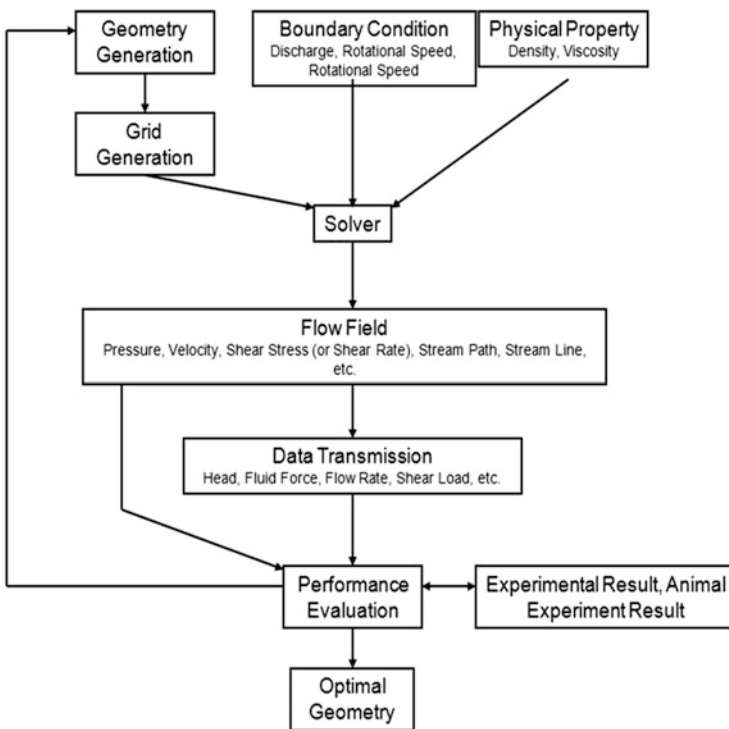
Fig. 13.8 Typical process of blood pump development using computational fluid dynamics (CFD) analysis

analysis (Antaki et al. 1995). The pump geometry is drawn using 3-D CAD software, and the meshes are generated as a result of discretization from the CAD geometry using grid-generation software. The flow is solved algebraically using CFD analysis software for the generated meshes by giving the physical properties of the fluid and the boundary conditions. Subsequently, the flow field and the fluid dynamic values translated from the flow field are calculated. Finally, the results are compared with the in vitro or in vivo experimental results, and the pump geometry is evaluated.

1. Geometry generation

The inner geometry is usually drawn using 3-D CAD software. The purpose of CFD analysis is to determine how precisely the geometry should be drawn, although it is well known that hemolytic and thrombogenic properties dramatically vary by the mere roundness of the edge (Umezu et al. 1992). There are different ways to solve the flows in the whole pump and those in a part of the pump. The way to solve the flow in a part of the pump requires a little effort and is effective when the purpose is clear, but the setting of the boundary conditions is usually difficult.

2. Grid generation

The produced inner geometry is divided into calculation meshes (Fig. 13.9) using commercial grid-generation software [Pointwise (Pointwise, USA), ICEM-CFD (ANSYS, USA), Turbogrid (ANSYS), etc.]. The high shear region in the vicinity of the wall surface, which is called a boundary layer, is divided into thin meshes comprising a prism mesh, etc. in a rotary blood pump. The comparably low shear region far from the wall surface is divided into thick meshes constituting a tetra mesh, etc. (Fig. 13.10). The number of meshes varies from 200,000 to more than 1,000,000 when solving the whole pump region. The number of meshes generated in the boundary layer is more important than that generated in the whole pump. Thus, the solution is usually conducted after the validation, for

Fig. 13.9 Meshes of a centrifugal blood pump for CFD analysis
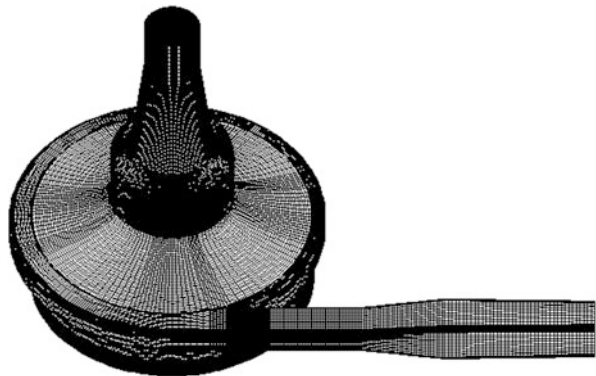
**Fig. 13.10** Connection of the *thin* and *thick* meshes

Far from the Wall:
Pyramid

Near the Wall:
Prism ($y^+ < 8$)
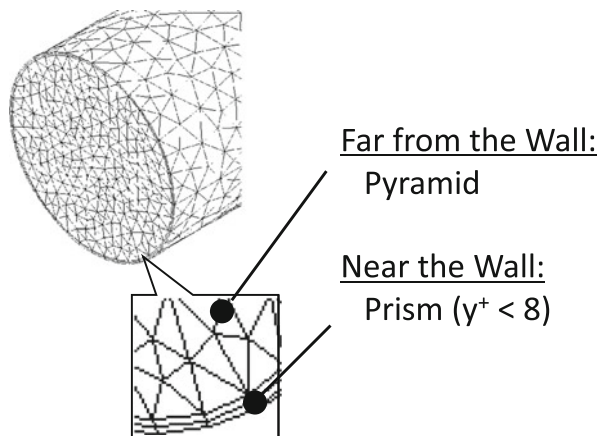
example, when checking the relationship between the number of meshes and the pump head (Qian 2004).

3. Solution

   The equations governing flow are algebraically solved using commercial analysis software [STAR-CCM+ (CD-Adapco, USA), Fluent (ANSYS), etc.] for generated meshes with physical properties and boundary conditions. Many studies use a finite volume method, which is the method most commonly used in commercial software, among some CFD methods, such as the differential method, finite volume method, finite element method, etc. Several studies have also used custom-written software, which sometimes achieves more precise analyses (Nakamura and Yano 1999). Commercial software is used because flow analyses in blood pumps need to be fast to be conducted in parallel with other experimental tests, such as tests of the pump performance, hemolytic properties, anti-thrombogenic properties, and fluidic force. The criteria for evaluating hemolytic and anti-thrombogenic properties are unclear, and there are many unstable factors in analyzing the flow when considering blood rheology, especially non-Newtonian and multiphase fluid dynamics that are actually almost impossible to solve. On the other hand, it is important to select the adequate turbulent model for accuracy. However, although there are many turbulent models, such as the laminar model, the k-ε model, and the large eddy simulation model, it is unclear which turbulent model is the most valid for the analysis of blood pumps. Generated meshes and turbulent models are simply validated by how much the performance curves calculated by the CFD analysis and those actually measured coincide (Fig. 13.11). These models have been recently validated by how much the velocity distributions calculated by CFD analysis and those actually measured coincide (Triep et al. 2006), although other problems with the accuracy of the velocity measurement arise. Furthermore, validation of the pressure distribution (Burgreen et al. 2001), stream path (Apel et al. 2001a), and turbulence component is required.

Fig. 13.11 Example of CFD validation using pump performance curve
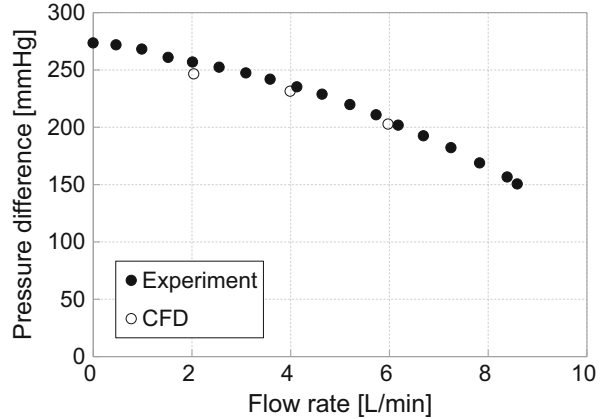
Fig. 13.12 Relationship between effective viscosity and shear rate (Wells et al. 1962)
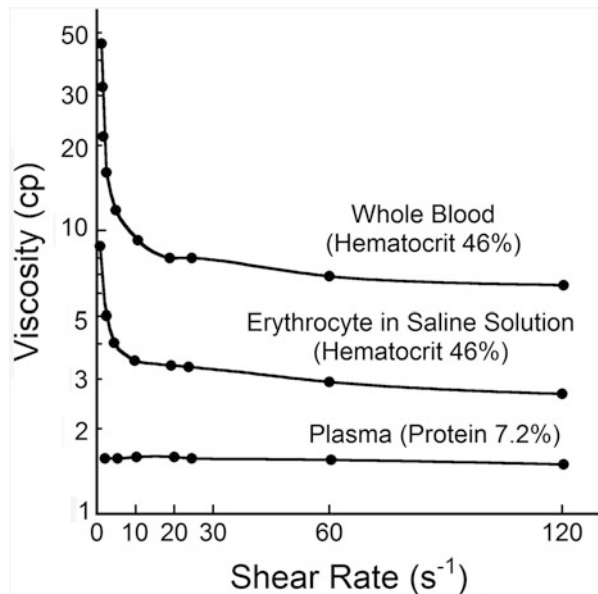
13.6.1.2 Blood Properties

Blood has a density of 1.056 kg/m^3 and a viscosity of 0.003 Pa · s (=3 cP, at 37 °C and in high shear flow) (Cooney 1976). The viscosity from 2.4 cP to 3.6 cP is adopted, and that of 3.5 cP is generally used for CFD analysis. One reason for various viscosities is differences between individuals, and another is that it depends on the high viscosity value in the low shear region because blood is a non-Newtonian fluid approximated to be a Casson fluid (Fig. 13.12) (Wells et al. 1962; Oka 1974). The fluid in the blood pump is approximated to be a Newtonian fluid in current flow analyses because there are high shear regions in almost all regions. Blood is also a multiphase fluid with hematocytes suspended in plasma, but

it is approximated to be continuous fluid for current flow analysis because the analysis considering multiphase properties is almost impossible in blood pumps. These effects should, however, be considered.

13.6.1.3 CFD of Pump Performance

The inner flow is analyzed to improve the pump performance of the blood pump, which is the same process as that in the fluid design of general pumps. The pump performance is evaluated by the pump head P, which is the pressure difference between the inlet and the outlet, as a function of the flow rate Q at the constant impeller rotational speed n.

In the 1990s, CFD was actively adapted for the design of axial-flow pumps, for which appropriate impeller design is difficult to determine (Butler et al. 1997). The analysis was then adapted for the design of centrifugal pumps (Chan et al. 2002), since the pump performance varies according to geometric factors such as the impeller geometry and the outlet position. The pump performance is the first property of blood pumps to be investigated because it also affects indirectly the hemolytic properties.

13.6.1.4 CFD of Hemolysis

Hemolysis is the rupture of erythrocytes. It is caused by fatigue failure resulting from repeated loading of high shear stress on the erythrocyte membrane in the blood pumps that sometimes exhibit excessive high shear regions. As well as the mechanism of the material fatigue failure, the amount of hemolysis is related to the shear stress and the number of loadings, that is, the exposure time (Fig. 13.13) (Helmus and Brown 1977). Thus, CFD of hemolysis is the analysis concerning the shear stress and the exposure time on erythrocytes. When the amount of hemolysis

Fig. 13.13 Relationship among hemolysis, shear stress, and exposure time (Helmus and Brown 1977)
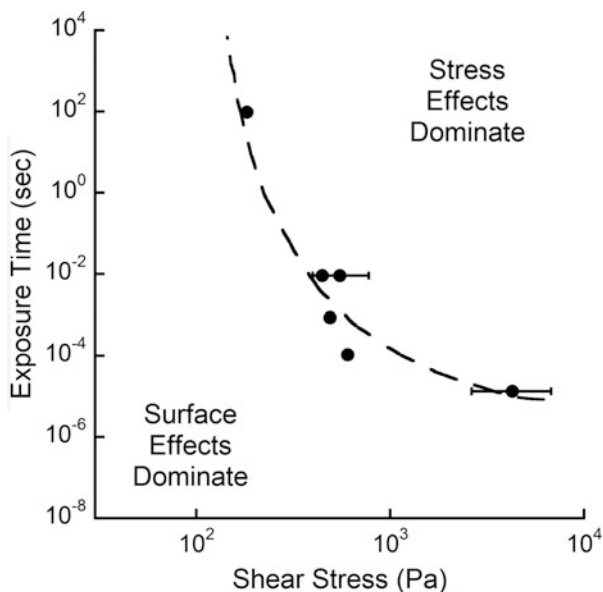
Table 13.7 Coefficients for hemolysis and shear stress (Blackshear et al. 1965; Heuser 1980; Wurzinger et al. 1985; Giersiepen et al. 1990; Song et al. 2004)

	Blackshear	Heuser	Giersiepen–Wurzinger
Blood	Canine	Porcine	Human
C	–	1.9×10^{-6}	3.62×10^{-5}
α	2	1.991	2.416
β	1	0.765	0.785
Range of τ and t	–	$40 < \tau < 700$	$57 < \tau < 255$
		$0.0034 < t < 0.6$	$0.007 < t < 0.7$

is dHb/Hb, the shear stress is τ, and the exposure time is t; their relationship is expressed by

$$\frac{dHb}{Hb} = C\tau^{\alpha}t^{\beta}, \tag{13.4}$$

where the coefficient C, and α and β, given in Table 13.7, were obtained from the results of shear loading experiments on blood using a rotational viscometer (Blackshear et al. 1965; Heuser 1980; Wurzinger et al. 1985; Giersiepen et al. 1990; Song et al. 2004). The shear stress history of an erythrocyte passing through artificial organs was first analyzed to understand the hemolysis of an artificial valve (Giersiepen et al. 1990). This technique was then adapted to understand the hemolysis of centrifugal blood pumps (Fig. 13.14) (Bludszweit 1995). Subsequently, this technique became a method for estimating hemolysis based on the shear stress for many particles (Mitamura et al. 2001).

The damage $d_{n,\,k}$ to an erythrocyte during the time interval $\Delta t_k(\,=t_k-t_{k-1})$ is expressed by

$$d_{n,k} = C\tau(t_{k-1})^{\alpha}\Delta t^{\beta}. \tag{13.5}$$

The damage $D_{n,k}$ to the erythrocyte between time 0 and t_k is expressed by

$$D_{n,k} = D_{n,k-1} + (1 - D_{n,k-1})d_{n,k}. \tag{13.6}$$

If the erythrocyte flows along the streamline, a shear stress history can be established. Here, the scalar shear stress τ

$$\tau = \sqrt{\frac{1}{6}\sum\left(\tau_{ii} - \tau_{jj}\right)^2 + \sum\tau_{ij}} \tag{13.7}$$

is usually used as shear stress, where τ_{ij} represents the shear stresses that are the sum of the viscous stress and the Reynolds stress. After the damage D_n of each erythrocyte is analyzed for each streamline from the inlet to the outlet of the pump, the average damage D passing through the pump is regarded as the estimated hemolysis. Many studies have examined the effect of shear stress and the exposure time for the hemolysis in the blood pump (Pinotti and Rosa 1995), whereas other
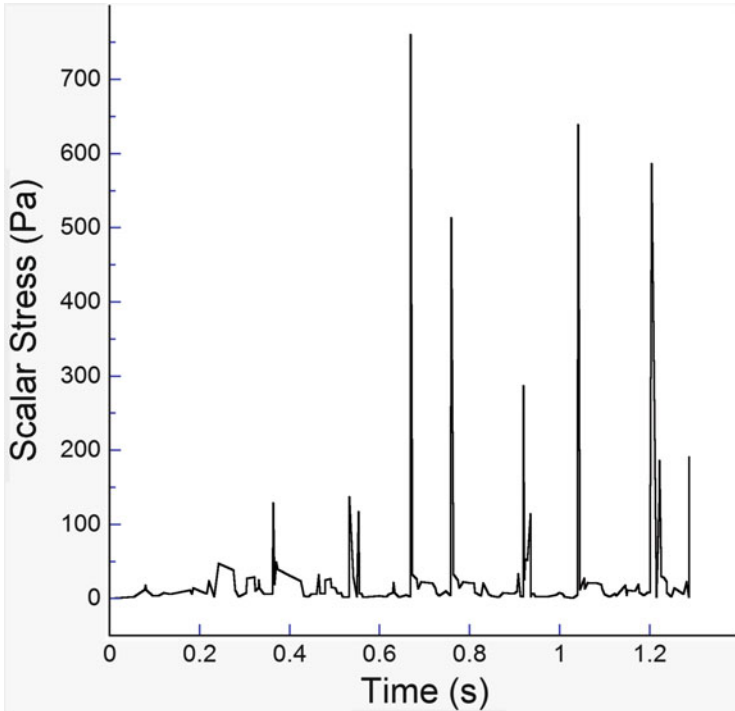
Fig. 13.14 Stress history of an erythrocyte in a centrifugal pump (Bludszweit 1995)

studies have examined additionally the effect of the pressure (Mizuguchi et al. 1995). Some earlier studies have analyzed the shear stress (Wood et al. 1999), and some studies have analyzed the relationship between the experimental results and hemolysis test results (Miyazoe et al. 1998). Various investigations have been conducted on hemolysis, including those on the effect of turbulence stress (Apel et al. 2001b), the effect of stretch (Arora et al. 2004), a method to estimate the volume integration of hemolysis (Garon and Farinas 2004), and the effect of the dissipation of the thrombocyte (Goubergrits and Affeld 2004).

13.6.1.5 CFD of Thrombus Formation

The mechanism of thrombus formation is more complicated than that of hemolysis. A thrombus is generally considered to be formed in a low shear region, that is, flow stagnation. It is sometimes formed in a narrow gap and by hemolysis. At present, CFD of thrombus formation is only analyzed by calculating the velocity distribution in the gap (Gobel et al. 2001; Tsukamoto et al. 2001; Burgreen et al. 2004) and shear stress (Nakamura et al. 1999; Nishida et al. 2006a). Figure 13.15 shows the example of geometric optimization of the blood pump using CFD analysis and anti-thrombogenicity. However, the estimation of thrombus formation by CFD is very important because the problem with blood pump development from a clinical perspective is thrombus formation.
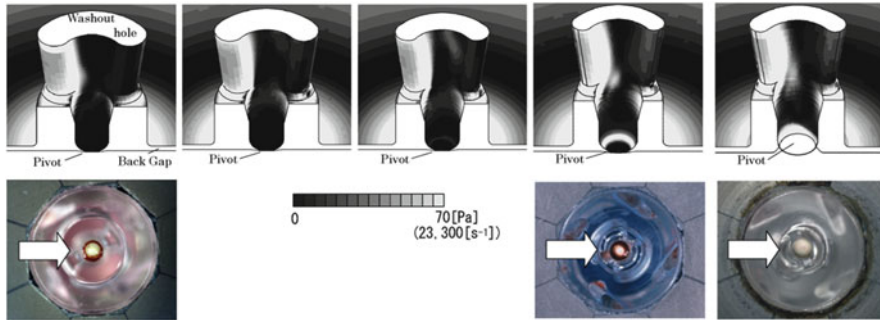
Fig. 13.15 Geometric optimization of the monopivot centrifugal pump using flow quantification and anti-thrombogenicity (Nishida et al. 2006a). *Upper* figures show CFD results for shear stress; *lower* figures show results of anti-thrombogenesis tests

### 13.6.1.6 CFD of Impeller Levitation

Some blood pumps do not have an impeller shaft to improve anti-thrombogenicity. Anti-thrombogenicity decreases at the gap between the seal and the shaft when the pump has an impeller shaft, and there are several kinds of pumps with pivot bearings, hydrodynamic bearings, magnetic bearings, etc. for supporting the impeller rotation. As the rotational position of the impeller is not necessarily fixed using these bearings, the analysis of fluid force on the impeller is important so the impeller does not touch the casing (Qian and Bertram 2000).

13.6.2 PIV Measurement

Although the PIV measurement, one of the experimental fluid dynamics analysis methods (Adrian and Westerweel 2011), is an effective tool to improve pump performance, and also to prevent hemolysis and thrombus formation, the PIV measurement or other experimental fluid dynamics analysis is usually regarded as a method to validate CFD analysis (Apel et al. 2001a). Namely, the PIV measurement is used to compensate for the accuracy of the CFD analysis. The development of a blood pump is now proceeding with a combination of the CFD analysis and experimental fluid dynamics analysis. In this section, the PIV measurement method of blood pumps in our laboratory is described.

13.6.2.1 Methodology of PIV

Figure 13.16 shows the experimental apparatus for flow visualization. Blood pumps are difficult to visualize because of their small size and the high rotational speed of the impeller. Thus, when developing blood pumps, selection of the scale model, working fluid, and image analysis requires several precautions. Namely, it is necessary to consider factors that affect the accuracy of the velocity measurement, for example, insufficient photographing speed of the video camera when visualizing
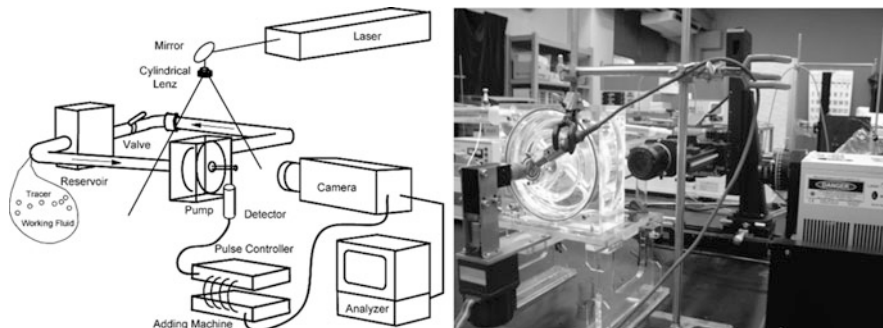
Fig. 13.16 Experimental apparatus for flow visualization

Table 13.8 Properties of the model scale

Pump model	Advantage	Disadvantage
Full-scale model	Low cost, small tasks	Low space resolution, low time resolution
Scale-up model	High space resolution, high time resolution	High cost, several tasks

full-scale models, the scaling error when visualizing scale models, and the total error when visualizing localized areas with high resolution.

1. Scale model

For a normal centrifugal blood pump, the impeller, whose overall diameter is approximately 50 mm, rotates at a speed of 2000 rpm. Thus, observation of overall flow is possible along with the impeller rotation if the flow is photographed using a full-scale model. However, flow analysis with greater precision and higher spatial resolution will be difficult because of the limits of photographing speed and optical magnification. In this case, a scale model makes it possible to increase the spatial and temporal resolution using the flow similarity law, but these types of models are expensive. Table 13.8 shows the properties of model scale.

The principle for a scale model is as follows (Stepanoff 1957). To be dynamically similar flow, the Reynolds number Re, which is the ratio of the inertial force to the viscous force,

$$Re = \frac{uR}{\nu} = \frac{2\pi R^2 N}{\nu} \tag{13.8}$$

and the flow rate coefficient ϕ, which is the geometry of the velocity triangle,

$$\phi = \frac{Q}{Au} = \frac{Q}{2\pi R^3 N} \tag{13.9}$$

coincide between a full-scale model and a scale model simultaneously, where R denotes the impeller radius, N the impeller rotational speed, ν the kinematic viscosity, Q the flow rate, A the representative area, and u the impeller tangential velocity. When the flow rate coefficient ϕ coincides between the two models, the head coefficient ψ

$$\psi = \frac{gH}{u^2} = \frac{gH}{R^2 N^2} \tag{13.10}$$

coincides between the two models. From Eq. (13.8), the impeller rotational speed in the scale model is given by

$$\frac{N_2}{N_1} = \left(\frac{R_1}{R_2}\right)^2 \times \frac{\nu_2}{\nu_1}. \tag{13.11}$$

where the subscript 1 indicates the value in the full-scale model, and the subscript 2 indicates the value in the scale model. From Eq. (13.9), the flow rate in the scale model is given by

$$\frac{Q_2}{Q_1} = \left(\frac{R_2}{R_1}\right)^3 \times \frac{N_2}{N_1} = \frac{R_2}{R_1} \times \frac{\nu_2}{\nu_1}. \tag{13.12}$$

From Eq. (13.10), the head in the scale model is given by

$$\frac{H_2}{H_1} = \left(\frac{R_2}{R_1}\right)^2 \times \left(\frac{N_2}{N_1}\right)^2. \tag{13.13}$$

From Eqs. (13.12) and (13.13), removing R gives

$$n_{S1} \equiv \frac{N_1 \sqrt{Q_1}}{H_1^{3/4}} = \frac{N_2 \sqrt{Q_2}}{H_2^{3/4}} \equiv n_{S2} \tag{13.14}$$

where n_s is defined as the specific speed. Therefore, to complete Eqs. (13.9) and (13.10), the specific speed n_s for the full-scale model and that for the scale model coincide.

2. Working fluid

Transparent fluids are used as the working fluid for the PIV measurement in the blood pump. Table 13.9 shows the physical properties of working fluids to simulate blood. These fluids include water, saline solution, glycerol solution, sodium iodide solution (Nishida et al. 1997), and a mixed solution of sodium iodide and glycerol

Table 13.9 Physical properties of working fluid to simulate blood (at room temperature, ≈20 °C)

	Specific gravity	(cSt)	Refractive index	(Advantage)	(Disadvantage)
Blood (37°C)	1.056	3 (or 3.5)	–		
Water	1	1	1.33	Easy handling	
Saline solution (5 wt% aq)	1.05	1. 03	N.A.	Easy handling, specific gravity matching	
Glycerol solution					
(40 wt% aq)	1.1	3.5	N.A.	Viscosity matching	
[100 %]	[1.26]	[1300]	[1.8]	[As a reference]	
Mixed solution of sodium iodide and glycerol					
(79 % saturated NaI aq + 20 % glycerin + 1%water)	1.75	3.8	1.49	Viscosity matching	Metal oxidation
(90 % saturated NaI aq +10 % glycerin)	1.87	3			
Sodium iodide solution (64 wt% aq)	1.9	1.8	1.49		Metal oxidation
Air	0.001	15	1	Easy handling	Visualization difficulty
Mineral oil	0.83	4.3–5.7	1.46		Flammable
Mixed solution of potassium thiocyanate and glycerol (56.4 KSCN w/o in 36 % glycerin aq)	1.43	3.5	1.49		Toxic

(Baldwin et al. 1994). Water, saline solution, and glycerol solution are easy to handle and are used to understand the overall flow. Saline solution is used to adjust the specific gravity, whereas glycerol solution is used to adjust the viscosity. However, because the refractive indices of these solutions are lower than that of acrylic resin (1.49), which is the general material for making pump models, the obtained images must be corrected to be quantified in the PIV measurement algorithm. It is not necessary to correct images if the refractive index of the working fluid coincides with that of acrylic resin. Sodium iodide solution (64 wt%, saturated) has the same refractive index as that of acrylic resin. Furthermore, a mixed solution of sodium iodide and glycerol has not only the same refractive index as acrylic resin but also the same kinematic viscosity as blood, which removes any

translation of physical properties using the full-scale model. However, the sodium iodide solution is usually better because it achieves a lower flow velocity resulting from a lower kinematic viscosity of the working fluid to increase the temporal resolution. Table 13.10 shows the physical properties of human whole blood, water, and 64 wt% sodium iodide solution, and experimental setting values expressed as multipliers to acquire the similar flow using a $3\times$ scale model versus the whole blood flow using a full-scale model.

3. Tracer particles

Various commercial tracer particles can be used for PIV measurements when the working fluid is water. However, the specific gravity of tracer particles should be large when the working fluid is 64 wt% sodium iodide solution, which has a specific gravity of 1.9. Silica particles have a specific gravity (1.9) identical to that of sodium iodide solution, and silver-coated hollow glass particles (specific gravity of 1.4) are commercially available. The silver-coated hollow glass particles are useful as tracer particles for the particle tracking method because of their good visibility.

4. Imaging system

Figure 13.17 shows the visualization regions in a centrifugal blood pump. Flow is periodic in a blood pump whether it is a continuous-flow or pulsatile-flow pump. Therefore, analyzing the flow in the blood pump is possible if a video camera can capture both continuous and periodic particle images. In our laboratory, the continuous particle images are firstly obtained to determine lens magnification and photographing speed. A large number of periodic particle images are then obtained by synchronizing constant impeller rotational phases. Finally, accuracy of the velocity measurement is improved by summation of the velocity data.
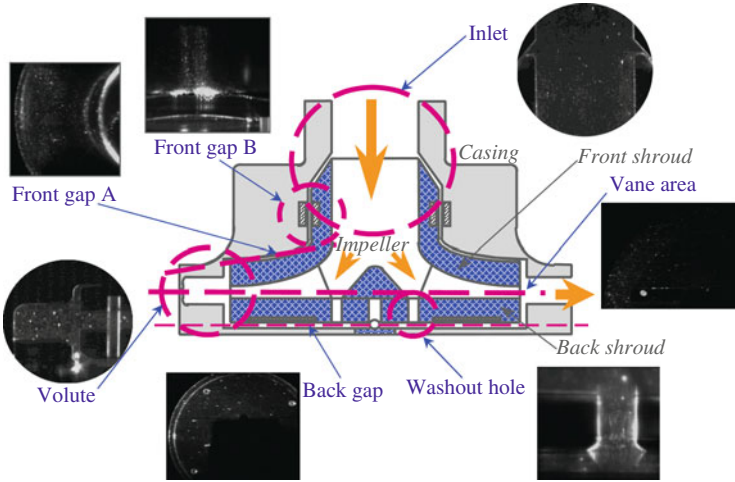
5. Image analysis

The PIV measurement method is generally classified into the particle tracking method and the correlation method, and both methods are used for the PIV measurement of the blood pump. In our laboratory, the four-frame particle tracking method (Kobayashi et al. 1989) is used to measure the flow in the vicinity of the wall surface with high spatial resolution. Figure 13.18 shows the flow visualization analysis results for various flows; the flow in the vicinity of the wall surface is important in blood pumps. The properties of both methods for the analysis of the flow in blood pumps are described as follows.
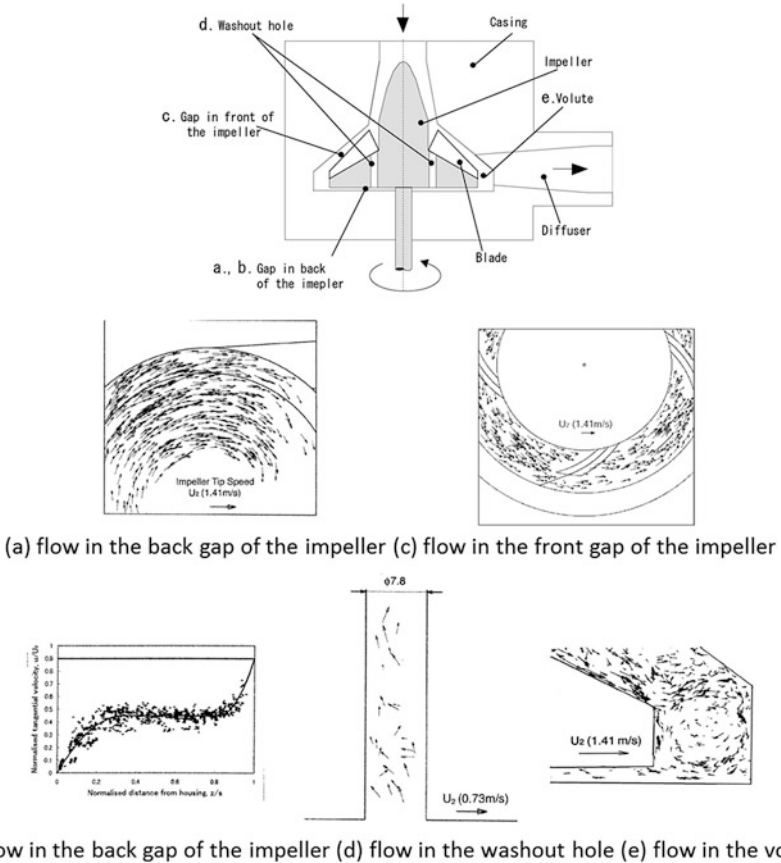
(a) Particle tracking method
    In the particle tracking method, velocity is calculated by the movement of a particle's centroid. Thus, the spatial resolution of the particle tracking method is high; it comprises point measurements. This method is better for measuring the flow in the vicinity of the wall precisely because particles hardly exist

Table 13.10 Physical properties of human whole blood, water, and 64 wt% sodium iodide solution, and experimental setting values expressed as multipliers to acquire the similar flow using a 3× scale model versus the whole blood flow using a full-scale model

Liquid	Physical property		Multiple of the setting value to be similar flow				
	Density $\rho \times 10^3$ kg/m^3	Kinematic viscosity $v \times 10^{-6}$ m^2/s	Length L (arbitrarily)	Velocity U ($\propto v$/L)	Rotational speed n (U/L)	Flow rate Q (UL^2)	Pressure P (ρU^2)
Human whole blood (at 37°C)	1.056	3	1	1	1	1	1
Water (at 20°C)	1	1	3	1/9	1/27	1	1/85.536
64 wt% NaI solution (at 20°C)	1.9	1.8	3	1/5	1/15	9/5	19/264

Fig. 13.17 Visualization regions in a centrifugal blood pump (Asztalos et al. 1999)

Fig. 13.18 Flow visualization analysis results for various flows

inside the flow, and the flow in the vicinity of the wall surface is important in the blood pump.

(b) Correlation method

In the correlation method, velocity is calculated as the average movement of particles in an interrogation area. Thus, the spatial resolution of the correlation method is lower than that of the particle tracking method and depends on the size of the interrogation area. However, the accuracy of the velocity is better than that of the particle tracking method because the velocity of the correlation method is an average velocity in the interrogation area.

6. Post analysis

The shear rate and the turbulence component are calculated from the velocity data obtained by the particle tracking method or the correlation method. The Reynolds stress and the shear stress are also calculated from the shear rate and the turbulence component.

13.6.2.2 PIV of Pump Performance

The important flow regions to be analyzed for the pump performance of blood pumps are the gap between impeller blades and near the cut-water, which locates from the impeller to the outlet. Figure 13.19 shows the example of the flow analysis of pump performance (Nishida et al. 1999). The flow in pumps with low pump performance sometimes causes a separation in the gap between the impeller blades and near the tongue. Thus, achieving smooth flow in a pump by improving the impeller geometry and outlet position results in a high-performance pump. However, the flow is rarely quantified for the pump performance because qualitative flow visualization is sufficient for observing the cause of the separation, as previously described.

13.6.2.3 PIV of Hemolysis

The amount of hemolysis is expressed as a function of the shear stress and the exposure time as shown in Eq. (13.4). High shear locates in the boundary layer in
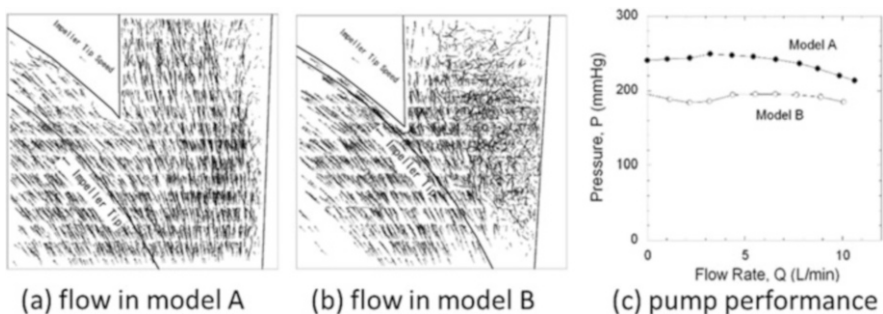

Fig. 13.19 Flow analysis of pump performance (Nishida et al. 1999)

the vicinity of the walls of the casing and the impeller in blood pumps where velocity is high or in the narrow gap. The thickness of the boundary layer is usually less than 100 μm in a centrifugal blood pump. The PIV measurement is a good method for quantifying the high shear in the boundary layer because the spatial resolution can be improved by adjusting the optical system. However, it is difficult to measure the exposure time for the shear, which makes it almost impossible to estimate the amount of hemolysis calculated by Eq. (13.4) experimentally. Figure 13.20 shows the relationship between high shear in the vicinity of the wall surface and hemolytic properties of tested pumps. At present, the PIV measurement is regarded as a reliable method to quantify the high shear in the boundary layer.
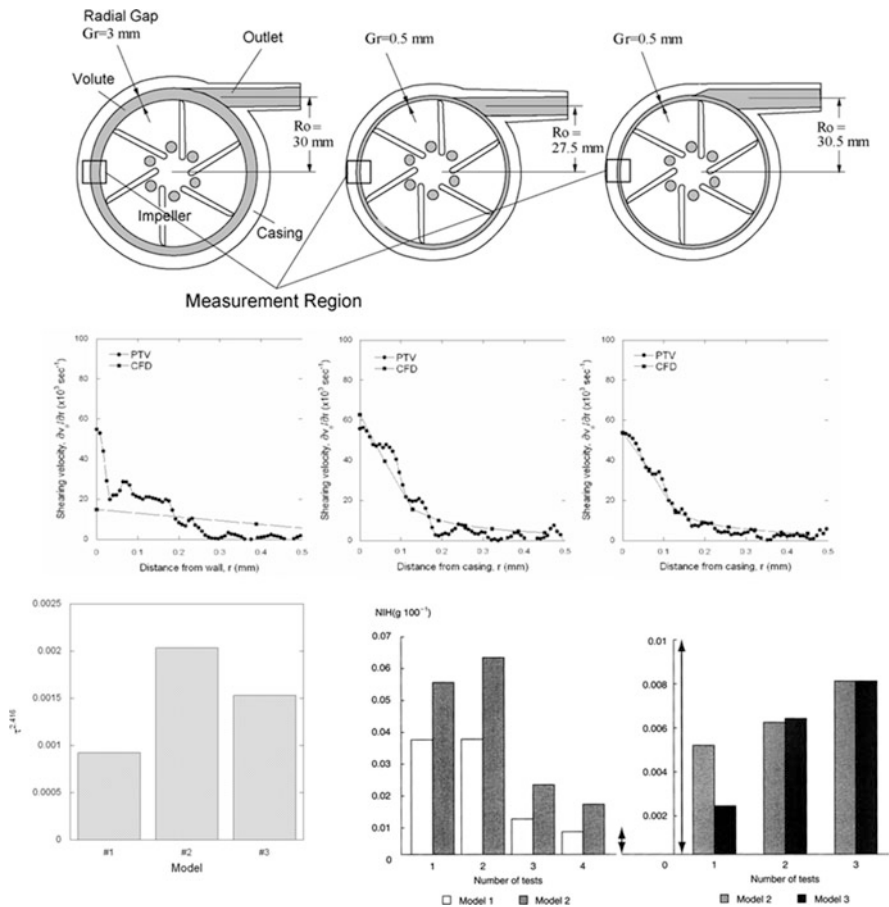
Fig. 13.20 Relationship between high shear in the vicinity of the wall surface and hemolytic properties of tested pumps (Nishida et al. 2006b). *Upper row*: pump geometries; *middle row*: shear rates; *lower row*: summations of shear stress $\tau^{2.416}$ and hemolysis test results)
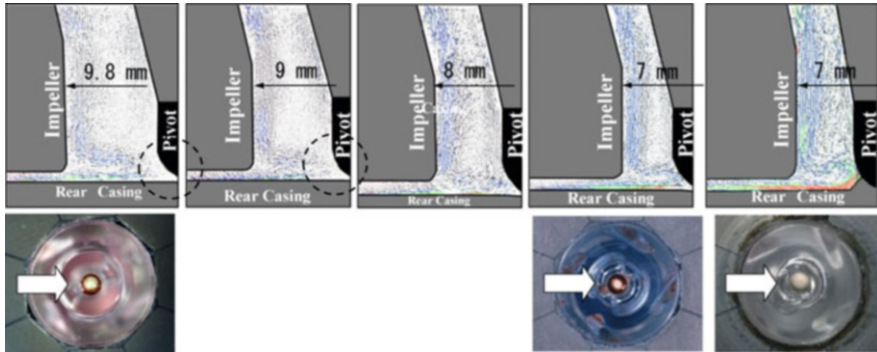
Fig. 13.21 Optimal design of the monopivot centrifugal pump using flow quantification and anti-thrombogenicity (Nishida et al. 1997). *Upper row*: PIV results; *lower row*: anti-thrombogenesis test results; *dotted circle*: stagnation region

13.6.2.4 PIV of Thrombus Formation

The mechanism of thrombus formation is more complex than that of hemolysis. The thrombus is generally considered to form in the low shear region, which is a region of flow stagnation, although it sometimes forms in the narrow gap and by hemolysis. Figure 13.21 shows the example of the optimal design of the blood pump using flow quantification and anti-thrombogenicity (Toyoda et al. 2002). If photographing particles is possible, the flow analysis of the stagnation region itself is not very difficult. However, it is usually difficult to photograph the flow in the stagnation region because it is located around the rotating axis.

13.7 Summary of This Chapter

This chapter presents current VADs and CPB pumps, their specifications, their classifications, and methods for designing and evaluating them, including flow analysis inside the pump to optimize the geometries. One particular VAD has exceeded 8 years of clinical durability and has provided a high quality of life for its wearers. In the future, VADs and CPB pumps will require enhanced performance and durability and will be adaptable to individual cases.

References

Adrian RJ, Westerweel J (2011) Particle image velocimetry. Cambridge University Press, New York

Affeld K et al (1976) New methods for the *in vitro* investigations of the flow patterns in artificial heart. Trans Am Soc Artif Intern Organs 22:460–467

Antaki JF et al (1995) Computational flow optimization of rotary blood pump components. Artif Organs 19(7):608–615

Apel J, Neudel F, Reul H (2001a) Computational fluid dynamics and experimental validation of a microaxial blood pump. ASAIO J 47(5):552–558

Apel J et al (2001b) Assessment of hemolysis related quantities in a microaxial blood pump by computational fluid dynamics. Artif Organs 25(5):341–347

Araki K, Taenaka Y, Masuzawa T et al (1993) A flow visualization study centrifugal blood pumps developed for long-term usage. Artif Organs 17(5):307–312

Arora D, Behr M, Pasquali M (2004) A tensor-based measure for estimating blood damage. Artif Organs 28(11):1002–1015

ASTM F1841-97 (1997) Standard practice for assessment of hemolysis in continuous flow blood pumps

Asztalos B, Yamane T, Nishida M (1999) Flow visualization analysis for evaluation of shear and recirculation in a new closed-type, monopivot centrifugal blood pump. Artif Organs 23 (10):939–946

Baldwin JT et al (1994) LDA measurements of mean velocity and Reynolds stress fields with in an artificial heart ventricle. J Biomech Eng 116:190–200

Blackshear PL, Dorman FD, Steinbach JH (1965) Some mechanical effects that influence hemolysis. Trans Am Soc Artif Intern Organs 11:112–120

Bludszweit C (1995) Three-dimensional numerical prediction of stress loading of blood particles in a centrifugal pump. Artif Organs 19(7):590–596

Burgreen GW, Antaki JF et al (2001) Computational fluid dynamics as a development tool for rotary blood pumps. Artif Organs 25(5):336–340

Burgreen GW et al (2004) Computational fluid dynamics analysis of a Maglev centrifugal left ventricular assist device. Artif Organs 28(10):874–880

Butler K, Thomas D, Antaki JF et al (1997) Development of the Nimbus/Pittsburgh axial flow left ventricular assist system. Artif Organs 21(7):602–610

Chan WK et al (2002) A computational study of the effects of inlet guide vanes on the performance of a centrifugal blood pump. Artif Organs 26(6):534–542

Chua LP et al (2002) Gap velocity measurements of a blood pump model. Artif Organs 26(8):682–694

Cooney DO (1976) Biomedical engineering principles. Dekker, New York

DeBakey ME (1934) A simple continuous flow blood transfusion instrument. New Orleans Med Surg J 87:386–389

Garon A, Farinas MI (2004) Fast three-dimensional numerical hemolysis approximation. Artif Organs 28(11):1016–1025

Gibbon JH Jr (1937) Artificial maintenance of circulation during experimental occlusion of pulmonary artery. Arch Surg 34:1150

Gibbon JH Jr, Miller BJ, Feinberg C (1953) An improved mechanical heart and lung apparatus. Med Clin N Am 37:1603

Giersiepen M, Wurzinger LJ et al (1990) Estimation of shear stress-related blood damage in heart valve prostheses: in vitro comparison of 25 aortic valves. Int J Artif Organs 13:300–306

Gobel C et al (2001) Development of the MEDOS/HIA DeltaStream extracorporeal rotary blood pump. Artif Organs 25(5):358–365

Golding LAR et al (1980) Chronic non-pulsatile blood flow in alive, awake animal 34-day survival. Trans Am Soc Artif Intern Organs 26:251–254

Goubergrits L, Affeld K (2004) Numerical estimation of blood damage in artificial organs. Artif Organs 28(5):499–507

Helmus JD, Brown CH (1977) Blood cell damage by mechanical forces. In: Hwang NHC, Normann NA (eds) Cardiovascular flow dynamics and measurement. University Park Press, Baltimore, pp 799–823

Heuser G (1980) A Couette viscometer for short time shearing of blood. Biorheology 17:17–24

Ikeda T, Yamane T et al (1996) A quantitative visualization study of flow in a scaled-up model of a centrifugal blood pump. Artif Organs 20(2):132–138

Imachi K, Mussivand T (2010) Outline of the International Organization for Standardization Standard for circulatory support devices. Artif Organs 34:695–698

ISO 14708–5 (2010) Implants for surgery: active implantable medical devices. Part 5: Circulatory support devices

ISO 5198 (1987) Centrifugal, mixed flow and axial flow pumps. Code for hydraulic performance tests: precision grade

Joyce DL, Joyce LD, Loebe M (eds) (2012) Mechanical circulatory support: principles and applications. McGraw-Hill, New York

Japan Society of Mechanical Engineers (ed) (1988) Fundamentals of computational fluid dynamics (in Japanese). Corona, Tokyo

Kawahito K, Nosé Y (1997) Hemolysis in different centrifugal pumps. Artif Organs 21:323–326

Kerrigan JP, Yamazaki K et al (1996) High-resolution fluorescent particle-tracking flow visualization within an intraventricular axial flow left ventricular assist device. Artif Organs 20 (6):534–540

Kobayashi T et al (1989) Velocity measurement of three -dimensional flow around rotating parallel disks by digital image processing. ASME FED 85:29–36

Kyo S (ed) (2014) Ventricular assist devices in advanced-stage heart failure. Springer, Heidelberg

Mitamura Y et al (2001) Prediction of hemolysis in rotary blood pumps with computational fluid dynamics analysis. J Congest Heart Fail Circ Support 1(4):331–336

Miyazoe Y et al (1998) Computational fluid dynamic analysis to establish design process of centrifugal blood pump. Artif Organs 22(5):381–385

Mizuguchi K et al (1995) Development of an axial flow ventricular assist device: in vitro and in vivo evaluation. Artif Organs 19(7):653–659

Nakamura S, Yano K (1999) Computational simulation of flows in an entire centrifugal heart pump. Artif Organs 23(6):572–575

Nakamura S et al (1999) Numeric flow simulation for an innovative ventricular assist system secondary impeller. ASAIO J 45(1):74–78

Nishida M, Yamane T et al (1997) Quantitative visualization of flow through a centrifugal blood pump: effect of washout holes. Artif Organs 21(7):720–729

Nishida M, Asztalos B, Yamane T et al (1999) Flow visualization study to improve hemocompatibility of a centrifugal blood pump. Artif Organs 23(8):697–703

Nishida M, Yamane T et al (2006a) Computational fluid dynamic analysis of the flow around the pivot bearing of the centrifugal ventricular assist device. JSME Int J Ser C 49(3):837–851

Nishida M et al (2006b) Quantitative Analysis of shearing velocity near the wall in a centrifugal blood pump, JSME Fluids Engineering Conference 2006 (CD-ROM): 812; 1–4

Oka S (1974) Biorheology (in Japanese). Shokabo, Tokyo

Pinotti M, Paone N (1996) Estimating mechanical blood trauma in a centrifugal blood pump: laser Doppler anemometer measurements of the mean velocity field. Artif Organs 20(6):546–552

Pinotti M, Rosa ES (1995) Computational prediction of hemolysis in a centrifugal ventricular assist device. Artif Organs 19(3):267–273

Pantalos GM et al (1998) Long-term mechanical circulatory support system reliability recommendation: American Society for Artificial Internal Organs and The Society of Thoracic Surgeons: long-term mechanical circulatory support system reliability recommendation. Ann Thorac Surg 66(5):1852–9.

Qian Y (2004) CFD application in Ventrassist implantable rotary blood pump design and validation. In: Proceedings, Bioengineering Conference Annual Meeting BED JSME, Kitakyushu, 22–23 January 2004, pp 259–260

Qian Y, Bertram CD (2000) Computational fluid dynamics analysis of hydrodynamic bearings of the VentrAssist rotary blood pump. Artif Organs 24(6):488–491

Rafferty EH et al (1968) Artificial heart II: application of nonpulsatile radially increasing pressure gradient pumping principle. Minn Med 51:191–193

Reul HM, Akdis M (2000) Blood pumps for circulatory support. Perfusion 15:295–311

Schima H et al (1992) Effect of stationary guiding vanes on improvement of the washout behind the rotor in centrifugal blood pumps. ASAIO J 38:220–224

Song X et al (2004) Quantitative evaluation of the blood damage in a centrifugal blood pump by computational fluid dynamics. J Fluids Eng 126(3):410–418

Stepanoff AJ (1957) Centrifugal and axial flow pumps, 2nd edn. Wiley, New York

Takatani S, Matsuda H, Hanatani A, Nojiri C, Yamazaki K, Motomura T, Ohuchi K, Sakamoto T, Yamane T (2005) Mechanical circulatory support devices (MCSD) in Japan: current status and future directions. J Artif Organs 8:13–27

Toyoda M et al (2002) Geometric optimization for non-thrombogenicity of a centrifugal blood pump through flow visualization. JSME Int J C45(4):1013–1019

Triep M et al (2006) Computational fluid dynamics and digital particle image velocimetry study of the flow through an optimized micro-axial blood pump. Artif Organs 30(5):384–391

Tsukamoto Y et al (2001) Computational fluid dynamics analysis for centrifugal blood pumps. J Congest Heart Fail Circ Support 1(4):337–343

Tsukiya T, Taenaka Y et al (2002) Improvement of washout flow in a centrifugal blood pump by a semi-open impeller. ASAIO J 48(1):76–82

Umezu M et al (1992) The effects of inter shapes of plastic connectors on blood in a extracorporeal circulation. In: Proceedings, 7th International Conference on Biomedical Engineering, Singapore, 2–4 December 1992, pp 197–199

Wells RE, Merrill EW, Gabelnick H (1962) Shear-rate dependence of viscosity of blood: interaction of red cells and plasma proteins. Trans Soc Rheol 6:19–24

Wood HG et al (1999) Numerical solution for blood flow in a centrifugal assist device. Int J Artif Organs 22(12):827–836

Wurzinger LJ et al (1985) Platelet and coagulation parameters following millisecond exposure to laminar shear stress. Thromb Haemost 54:381–386

Yamane T (2002) The present and future state of nonpulsatile artificial heart technology. J Artif Organs 5:149–155

Yamane T et al (2010) Japanese guidance for ventricular assist devices/total artificial hearts. Artif Organs 34:699–702